

SYNTHETIC GENETIC ARRAY (SGA) ANALYSIS IN *SACCHAROMYCES CEREVISIAE* AND *SCHIZOSACCHAROMYCES POMBE*

Anastasia Baryshnikova,^{*} Michael Costanzo,^{*} Scott Dixon,[†]
Franco J. Vizeacoumar,^{*} Chad L. Myers,^{*} Brenda Andrews,^{*}
and Charles Boone^{*}

Contents

1. Introduction	146
2. Methodology	148
2.1. SGA query strain construction	148
2.2. Pin tool sterilization procedures	150
2.3. Constructing a 1536-density DMA	152
2.4. SGA procedure	153
2.5. Double mutant array image acquisition and processing	155
2.6. Quantitative scoring of genetic interactions using colony size-based fitness measurements	157
2.7. Interpretation and analysis of genetic interactions	159
2.8. <i>S. pombe</i> SGA	165
3. Media and Stock Solutions	168
3.1. SGA media and stock solutions	168
3.2. <i>Sp</i> SGA media and stock solutions	171
4. Applications of SGA Methodology	171
4.1. Integrating SGA and high-content screening	171
4.2. Essential gene and higher order genetic interactions	174
4.3. Combining SGA and gene overexpression libraries	174
4.4. Applying SGA as a method for high-resolution genetic mapping (SGAM)	175
4.5. Chemical genomics	175
References	176

^{*} Banting and Best Department of Medical Research and Department of Molecular Genetics, Terrence Donnelly Center for Cellular and Biomolecular Research, University of Toronto, Toronto, Ontario, Canada

[†] Department of Biological Sciences, Columbia University, New York, New York, USA

^{*} Department of Computer Science and Engineering, University of Minnesota-Twin Cities, Minneapolis, Minnesota, USA

Abstract

A genetic interaction occurs when the combination of two mutations leads to an unexpected phenotype. Screens for synthetic genetic interactions have been used extensively to identify genes whose products are functionally related. In particular, synthetic lethal genetic interactions often identify genes that buffer one another or impinge on the same essential pathway. For the yeast *Saccharomyces cerevisiae*, we developed a method termed synthetic genetic array (SGA) analysis, which offers an efficient approach for the systematic construction of double mutants and enables a global analysis of synthetic genetic interactions. In a typical SGA screen, a query mutation is crossed to an ordered array of ~ 5000 viable gene deletion mutants (representing $\sim 80\%$ of all yeast genes) such that meiotic progeny harboring both mutations can be scored for fitness defects. This approach can be extended to all ~ 6000 genes through the use of yeast arrays containing mutants carrying conditional or hypomorphic alleles of essential genes. Estimating the fitness for the two single mutants and their corresponding double mutant enables a quantitative measurement of genetic interactions, distinguishing negative (synthetic lethal) and positive (within pathway and suppression) interactions. The profile of genetic interactions represents a rich phenotypic signature for each gene and clustering genetic interaction profiles group genes into functionally relevant pathways and complexes. This array-based approach automates yeast genetic analysis in general and can be easily adapted for a number of different genetic screens or combined with high-content screening systems to quantify the activity of specific reporters in genome-wide sets of single or more complex multiple mutant backgrounds. Comparison of genetic and chemical-genetic interaction profiles offers the potential to link bioactive compounds to their targets. Finally, we also developed an SGA system for the fission yeast *Schizosaccharomyces pombe*, providing another model system for comparative analysis of genetic networks and testing the conservation of genetic networks over millions of years of evolution.

1. INTRODUCTION

A genetic interaction refers to an unexpected phenotype not easily explained by combining the effects of individual genetic variants (Bateson *et al.*, 1905). Importantly, genetic interactions organize into complex networks that may underlie the relationship between an organism's genotype and its phenotype (Waddington, 1957). Thus, an unbiased, systematic analysis of these networks and the interactions that comprise them is required in order to understand the genetic basis underlying disease. Given the complexity of the human genome (Levy *et al.*, 2007), determining how different alleles and polymorphisms combine to manifest a phenotype is a daunting task. Researchers have, therefore, embraced inbred model systems as well as isogenic populations of cultured cells derived from fruit

flies and mammals, as platforms to map genetic interactions in a systematic, unbiased, and comprehensive fashion (Dixon *et al.*, 2009).

Large-scale genetic interaction mapping studies were pioneered in *Saccharomyces cerevisiae* and focused on the identification of a specific type of interaction termed synthetic lethality (Tong *et al.*, 2001, 2004). Synthetic lethal or sick interactions, in which a combination of mutations in two genes results in cell death or reduced fitness, respectively, has been used extensively in different model organisms to identify genes whose products buffer one another and impinge on the same essential biological process (Fay *et al.*, 2002; Hartman *et al.*, 2001; Lucchesi, 1968). Genome-wide synthetic lethal analysis in yeast revealed the importance of systematic genetic interaction maps for assessing the biological roles of genes *in vivo* and uncovering new components of specific pathways (Pan *et al.*, 2006; Tong *et al.*, 2004). Recently, genetic mapping technologies combined with quantitative phenotypic analyses have enabled further dissection of genetic interactions into different types and classes offering the potential to define protein complex membership and infer order of gene function within specific biochemical pathways (Collins *et al.*, 2006; St Onge *et al.*, 2007).

The first enabling reagent set for large-scale genetic interaction screens in budding yeast was derived from the deletion mutant project, in which each known or suspected open reading frame is deleted and replaced with the dominant drug-resistance marker, *kanMX* (Giaever *et al.*, 2002; Winzeler *et al.*, 1999). The international consortium responsible for this landmark analysis identified ~1000 essential genes and constructed ~5000 viable haploid deletion mutants. The introduction of molecular tags or barcodes, a unique 20-bp DNA sequence at either end of the deletion cassette, acts as a unique mutant strain identifier enabling the fitness of a particular mutant to be assessed within a population using a barcode microarray (Giaever *et al.*, 1999). Additional libraries have subsequently been developed in which each of the ~1000 essential genes are altered in such a way as to produce either conditional alleles (Ben-Aroya *et al.*, 2008; Mnaimneh *et al.*, 2004) or hypomorphic (partially functional) alleles compatible with viability (Schuldiner *et al.*, 2005). Combining the viable deletion mutant and essential gene mutant collections provides the first opportunity for systematic genetic analysis in yeast and the potential for examining the complete genome-wide set of ~18 million different double mutants for synthetic genetic interactions.

Synthetic genetic array (SGA) analysis enables the systematic construction of double mutants (Tong *et al.*, 2001), allowing large-scale mapping of synthetic genetic interactions (Costanzo *et al.*, submitted for publication; Tong *et al.*, 2004). A typical SGA screen involves crossing a “query” strain to the array of ~5000 viable deletion mutants, but the array may also include essential gene mutants, and through a series of replica-pinning procedures, the double mutants are selected and scored for growth.

Applying SGA analysis on a genome-wide scale to ~ 1700 query mutations has enabled us to generate a genetic interaction network containing $\sim 170,000$ interactions, with functional information associated with the position and connectivity of a gene on the network (Costanzo *et al.*, submitted for publication).

The SGA methodology is versatile because any genetic element (or any number of genetic elements) linked to a selectable marker(s) can be manipulated similarly. In this regard, SGA methodology automates yeast genetics generally, such that specific alleles of genes, including point mutants and temperature-sensitive alleles, or plasmids can be crossed into any ordered array of strains providing systematic approaches to genetic suppression analysis, dosage lethality, dosage suppression or plasmid or reporter shuffling. In this chapter, we describe the steps of SGA analysis in detail and we hope to encourage laboratories from a broad spectrum of fields to adopt this methodology to suit their specific interests.



2. METHODOLOGY

SGA analysis first requires a relatively simple set up, generating the query strains and the array strains, and then the procedure itself basically involves several replica-plating steps, which are amenable to either manual or robotic manipulation. Each step of the procedure is described in detail below.

- SGA query strain construction
- Pin tool sterilization procedures
- Constructing a 1536-density deletion mutant array (DMA)
- SGA procedure
- Double mutant array image acquisition and processing
- Quantitative scoring of genetic interactions using colony size-based fitness measurements
- Interpretation and analysis of genetic interactions

2.1. SGA query strain construction

As mentioned above, SGA enables high-throughput construction and isolation of haploid double mutants by mating a “query” strain of interest harboring SGA reporters to an ordered array of mutant strains. This section describes different approaches for constructing SGA query strains.

2.1.1. Nonessential query strain: PCR-mediated gene deletion

1. Synthesize two gene-deletion primers, each containing 55 bp of sequence at the 5' end that is specific to the region upstream or downstream of the gene of interest (*Gene X*), excluding the start and stop codons and 22 bp of sequence at the 3' end that is specific for the amplification of the *natMX4* cassette (Goldstein and McCusker, 1999). The *MX4* cassette amplification sequences include the forward amplification primer (5'-ACATG-GAGGCCCAAGTACCCT-3') and the reverse amplification primer (5'-CAGTATAGCGACCAGCATTCAC-3').
2. Set up a 100 μ l PCR reaction (68.7 μ l H₂O, 10 μ l 10 \times PCR buffer, 2 μ l 10 mM dNTPs, 2 μ l 50 μ M forward primer, 2 μ l 50 μ M reverse primer, \sim 0.1 μ g p4339 DNA template in 10 μ l, 5 μ l DMSO, 0.3 μ l 5 U/ μ l Taq polymerase) to amplify the *natMX4* cassette flanked with 55-bp target sequences from p4339 (pCRII-TOPO::*natMX4*) with the gene-deletion primers designed in step 1. Plasmid p4339 serves as a DNA template to amplify the *natMX4* cassette.
3. Cycle as follows in a thermocycler with a heated lid: 95 $^{\circ}$ C 5 min, 95 $^{\circ}$ C 30 s, 55 $^{\circ}$ C 30 s, 68 $^{\circ}$ C 2 min, repeat 30 times, 68 $^{\circ}$ C 10 min, hold at 4 $^{\circ}$ C. PCR products can be stored at -20° C.
4. Transform the PCR product into the SGA starting strain, Y7092 (*MAT α can1 Δ ::STE2pr-Sp_his5 lyp1 Δ ura3 Δ 0 leu2 Δ 0 his3 Δ 1 met15 Δ 0*) using standard procedures (Winzeler *et al.*, 1999). Y7092 harbors reporters and markers necessary for SGA haploid strain selection following meiotic recombination. In particular, the *MAT α* -specific reporter [*STE2pr-Sp_his5*, composed of the *Saccharomyces cerevisiae* *STE2* promoter driving the *Schizosaccharomyces pombe* *his5* gene, which complements *S. cerevisiae* *his3 Δ 1* (Tong and Boone, 2006)] was integrated at the *CAN1* locus. Loss of *CAN1* confers canavanine resistance. Y7092 also carries a *lyp1* marker, which confers resistance to thialysine. The *can1* and *lyp1* mutations serve as recessive counterselectable markers designed to remove unwanted heterozygous diploids from the population. Select transformants on YEPD + clonNAT medium (see Section 3).

2.1.2. Nonessential query strain: Gene deletion marker switch method

1. Obtain the deletion strain of interest (*xxx Δ ::kanMX4*) from the *MAT α* deletion collection (OpenBiosystems), mate with Y8205 (*MAT α can1 Δ ::STE2pr-Sp_his5 lyp1 Δ ::STE3pr-LEU2 ura3 Δ 0 leu2 Δ 0 his3 Δ 1*) and isolate diploid zygotes by micromanipulation. Transform the resulting diploid with *Eco*RI-digested p4339 (see above) using standard yeast transformation protocols (Winzeler *et al.*, 1999). This procedure switches the gene deletion marker from *kanMX4* to *natMX4*. Select transformants on YEPD + clonNAT medium (see Section 3).

2. Transfer the resultant diploids to enriched sporulation medium (see [Section 3](#)) and incubate at 22 °C for 5 days.
3. A *MAT α* -specific reporter (*STE3pr-LEU2*) was integrated at the *LYP1* locus in Y8205 to provide a convenient method for selecting *MAT α* meiotic progeny. Resuspend a small amount of spores in sterile water and grow on SD – Leu/Lys/Arg + canavanine/thialysine (see [Section 3](#)) to select *MAT α* meiotic progeny. Incubate at 30 °C for ~2 days. To facilitate the selection of *MAT α* meiotic progeny we aim to plate ~200–300 colonies.
4. Replica plate to YEPD + clonNAT (see [Section 3](#)) to identify the *MAT α* meiotic progeny that carry the query deletion marked with *natMX4* (*xxx Δ ::natMX4*).

2.2. Pin tool sterilization procedures

The SGA procedure involves sequential transfer of yeast colonies onto different selective media in order to isolate haploid double mutant strains. Yeast colony transfer is accomplished manually using hand-held pin tools or automatically using robotically controlled pin tools. The following section describes pin tool sterilization procedures for both manual and robotic devices.

2.2.1. Manual pin tools (for low throughput: ~1–2 genome-wide screens/month)

The following manual pin tools can be purchased from V&P Scientific, Inc. (San Diego, CA): 96 floating pin E-clip style manual replicator (VP408FH), 384 floating pin E-clip style manual replicator (VP384F), Registration accessories: Library CopierTM (VP381), Colony CopierTM (VP380), Pin cleaning accessories: plastic bleach or water reservoirs (VP421), pyrex alcohol reservoir with lid (VP420), pin cleaning brush (VP425).

1. Set up the wash reservoirs as follows: three trays of sterile water of increasing volume—30, 50, and 70 ml, one tray of 40 ml of 10% bleach, one tray of 90 ml of 95% ethanol. To ensure that pins are cleaned properly and to avoid contamination in the wash procedure, the volume of wash liquids in the cleaning reservoirs is calculated to cover the pins sequentially in small increments. For example, only the tips of the pins should be submerged in water in the first step. As the pins are transferred to subsequent cleaning reservoirs and the final ethanol step, the lower halves of the pins should be covered.
2. Let the replicator sit in the 30 ml-water reservoir for ~1 min to remove the cells on the pins.
3. Place the replicator in 10% bleach for ~20 s.

4. Transfer the replicator to the 50 ml-water reservoir and then to the 70 ml-water reservoir to rinse the bleach off the pins.
5. Transfer the replicator to 95% ethanol.
6. Let excess ethanol drip off the pins, then flame.
7. Allow replicator to cool.
8. The manual replicator tools are compatible with OmniTray (Nunc) petri dishes. We found that ~ 35 ml of media in OmniTrays yield optimal results.

2.2.2. Singer RoToR bench top robot (for high-throughput SGA analysis)

The Singer RoToR can be purchased from Singer Instruments (Somerset, UK; www.singerinst.co.uk). This system uses disposable plastic replicators (RePads, Singer Instruments, UK) and thus does not require any sterilization procedures, making it simple and rapid to use. The Singer RoToR HDA bench top robot also uses PlusPlate (Singer Instruments) petri dishes that have a larger surface area but the same external footprint dimensions as OmniTray (Nunc). These larger plates facilitate replica-plating with the disposable RePads. We found that ~ 50 ml of media in PlusPlates yield optimal results.

2.2.3. BioMatrix robot (for ultrahigh-throughput SGA analysis)

The BioMatrix Colony Arrayer Robot can be purchased from S&P Robotics, Inc. (Toronto, ON; www.sprobotics.com). Use the following procedure to clean and sterilize the replicator pins prior to use of the robot:

1. Fill the sonicator bath with 390 ml sterile distilled water.
2. Clean the replicator pins in the sonicator for 5 min.
3. Remove the water and fill the sonicator bath with 390 ml 70% ethanol.
4. Sterilize the replicator in the sonicator for 20 s per cycle, repeat the cycle twice.
5. Let the replicator sit in a tray of 100 ml of 95% ethanol for 5 s.
6. Allow the replicator to dry over the fan for 20 s.

Use the following procedure to sterilize the pins at the end of each replica pinning step:

1. Set up the wash reservoirs as follows: Program water bath to automatically fill with sterile distilled water from bottle supply source, manually fill brush station with 320 ml sterile distilled water, fill sonicator with 390 ml 70% ethanol and basin with 100 ml 95% ethanol.
2. Let the replicator sit in the water bath for 10 s per cycle, repeat the cycle for four additional times to remove residual cells from replicator pins.
3. Clean replicator pins further at the brush station for three cycles.

4. Sterilize the replicator in the 70% ethanol-sonicator bath for 20 s per cycle, repeat twice.
5. Let the replicator sit in the 95% ethanol reservoir for 5 s.
6. Allow the replicator to dry over the fan for 20 s.
7. The BioMatrix robot can be used in conjunction with OmniTray (Nunc) petri dishes for the replica pinning steps involved in SGA analysis.

2.3. Constructing a 1536-density DMA

The collection of *MATa* deletion strains is available in stamped 96-well agar or frozen stocks in 96-well plates from various sources (Invitrogen, American Type Culture Collection, EUROSCARF, and Open Biosystems). However, deletion strains are arrayed at a higher density for SGA analysis. Specifically, each SGA array plate consists of 384 mutant strains arrayed in quadruplicate resulting in an array density of 1536 yeast colonies/plate. The following section describes how to assemble high-density SGA arrays from low-density (96 colonies/plate) source arrays available from different suppliers. The procedure described here employs a BioMatrix Colony Arrayer Robot but high-density DMAs can also be assembled using manual pin tools or the Singer RoToR instrument.

1. Peel off the foil coverings slowly on the frozen 96-well microtiter plates.
2. Let the plates thaw completely on a flat surface.
3. Mix the glycerol stocks gently by stirring with a 96-pin replicator.
4. Replicate the glycerol stocks from the 96-well plates onto YEPD + G418 agar plates using the Library CopierTM with the pair of one-alignment holes on the front frame. Take extreme caution that the pins do not drip liquid into neighboring wells.
5. Reseal the 96-well plates with fresh aluminum sealing tape and return to -80°C .
6. Let cells grow at room temperature for ~ 2 days.
7. Condense four plates of 96-format into one plate of 384-format using the BioMatrix Colony Arrayer Robot 96-pin replicator and the accompanying BioMatrix replicator software.
8. Incubate 384-density arrays at room temperature for ~ 2 days.
9. Replicate each 384-density DMA in quadruplicate onto a single plate using the BioMatrix robot 384-pin replicator and accompanying BioMatrix replicator software. This will generate a DMA consisting of 384 mutant strains and 1536 yeast colonies.
10. Incubate at room temperature for ~ 2 days, to generate a 1536-density DMA working copy.

2.4. SGA procedure

The following section provides a detailed description of the six steps involved in SGA-mediated double mutant isolation. The media required for various selections are described in detail in [Section 3](#). A schematic illustrating the SGA procedure is shown in [Fig. 7.1](#).

2.4.1. Query strain and DMA

1. Grow the query strain in a 5 ml YEPD overnight culture.
2. Pour the query strain culture onto a YEPD plate, use the replicator to transfer the liquid culture onto two fresh YEPD plates, generating a source of newly grown query cells for mating to the DMA in the density of 1536 colonies. Pinning the query strain in a 1536-format on an agar plate is advantageous as cells are evenly transferred to subsequent mating steps. One query plate should contain a sufficient amount of cells for mating with eight plates of the DMA. Allow cells to grow at 30 °C for 2 days.
3. Replicate the DMA to fresh YEPD + G418 media. Allow cells to grow at 30 °C for 1 day. The DMA can be reused for three to four rounds of mating reactions.

2.4.2. Mating the query strain with the DMA

1. Pin the 1536-format query strain onto a fresh YEPD plate.
2. Pin the DMA on top of the query cells.
3. Incubate the mating plates at room temperature for 1 day.

2.4.3. *MATa*/ α diploid selection and sporulation

1. Pin the resulting *MATa*/ α zygotes onto YEPD + G418/clonNAT plates.
2. Incubate the diploid selection plates at 30 °C for 2 days.
3. Pin diploid cells onto enriched sporulation medium.
4. Incubate the sporulation plates at 22 °C for 5 days.

2.4.4. *MATa* meiotic progeny selection

1. Pin spores onto SD – His/Arg/Lys + canavanine/thialysine plates.
2. Incubate the haploid selection plates at 30 °C for 2 days.

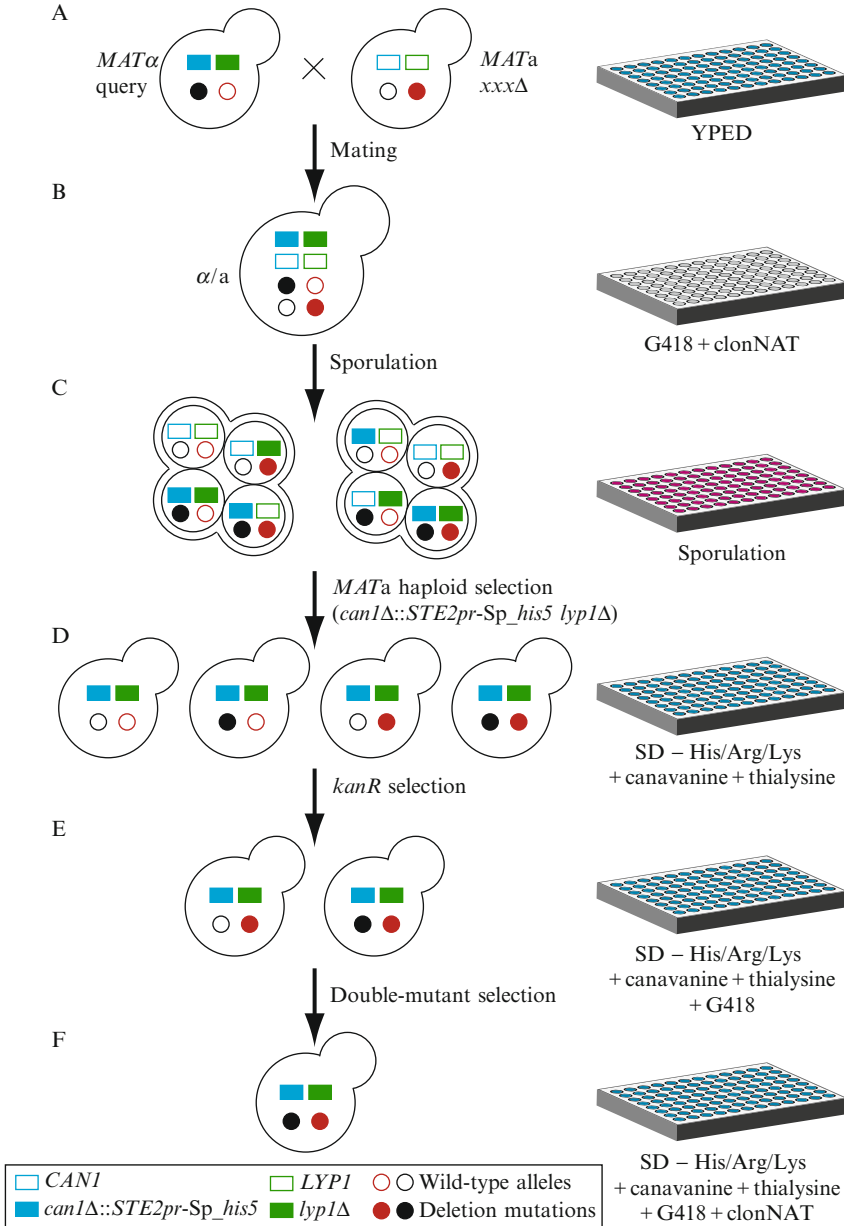


Figure 7.1 Synthetic genetic array (SGA) methodology. (A) A *MATα* strain carries a query mutation linked to a dominant selectable marker (filled black circle), such as the nourseothricin-resistance marker, *natMX4*, and the SGA reporter, *can1Δ::STE2pr-Sp_his5* (in which *STE2pr-Sp_his5* is integrated into the genome such that it deletes the open reading frame (ORF) of the *CAN1* gene, which normally confers sensitivity

2.4.5. *MATa-kanMX4* meiotic progeny selection

1. Pin the *MATa* meiotic progeny onto (SD/MSG) – His/Arg/Lys + canavanine/thialysine/G418 plates.
2. Incubate the *kanMX4*-selection plates at 30 °C for 2 days.

2.4.6. *MATa-kanMX4-natMX4* meiotic progeny selection

1. Pin the *MATa* meiotic progeny onto (SD/MSG) – His/Arg/Lys + canavanine/thialysine/G418/clonNAT plates.
2. Incubate the *kanMX4/natMX4* selection plates at 30 °C for 1–2 days.
3. Image double mutant array plates and score for fitness defect. The barcode microarrays can be used as an alternative method to score double mutants for fitness defects. Since each of the deletion mutants is tagged with two unique oligonucleotide barcodes, their growth rates can also be monitored within a population of cells (Decourty *et al.*, 2008; Pan *et al.*, 2004).

2.5. Double mutant array image acquisition and processing

Initial SGA screens focused on detecting severe synthetic sick or synthetic lethal interactions via visual inspection of double mutant colonies and comparison to wild-type controls (Tong *et al.*, 2001, 2004). However, quantitative measurement of genetic interactions offers the potential for constructing high-resolution genetic networks (Collins *et al.*, 2006; St Onge *et al.*, 2007). We developed an automated computational pipeline for acquiring and processing yeast colony data to extract precise fitness and genetic interaction measurements from yeast double mutant colony size (Fig. 7.2) (Baryshnikova *et al.*, manuscript in preparation; Tong *et al.*, 2004).

to canavanine). The query strain also lacks the *LYP1* gene. Deletion of *LYP1* confers resistance to thialysine. This query strain is crossed to an ordered array of *MATa* deletion mutants (*xxxΔ*). In each of these deletion strains, a single gene is disrupted by the insertion of a dominant selectable marker, such as the kanamycin-resistance (*kanMX4*) module (the disrupted gene is represented as a filled red circle). (B) The resulting heterozygous diploids are transferred to a medium with reduced carbon and nitrogen to induce sporulation and form haploid meiotic spore progeny. (C) Spores are transferred to a synthetic medium that lacks histidine, which allows selective germination of *MATa* meiotic progeny owing to the expression of the SGA reporter, *can1Δ::STE2pr-Sp_his5*. To improve this selection, canavanine and thialysine, which select *can1Δ* and *lyp1Δ* while killing *CAN1* and *LYP1* cells, respectively, are included in the selection medium. (D) The *MATa* meiotic progeny are transferred to a medium that contains kanamycin which selects single mutants equivalent to the original array mutants and double mutants. (E, F) An array of double mutants is selected on a medium that contains both nourseothricin and kanamycin.

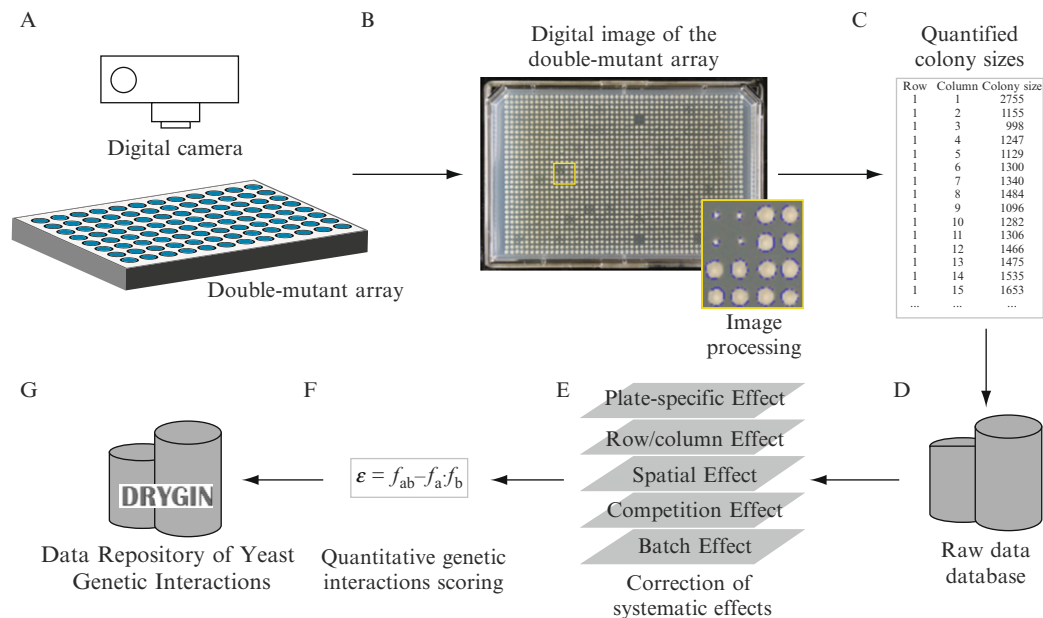


Figure 7.2 Computational pipeline for processing SGA data. (A) Double mutant array plates are photographed by a high-resolution digital camera. (B, C) Digital images of the double mutant array plates are processed by a custom-developed image processing software that identifies the colonies and measures their areas in terms of pixels. (D) Quantified double mutant colony sizes are stored in the database for further manipulation and analysis. (E) To identify quantitative genetic interactions, the yeast colony data is retrieved from the database and a series of normalizations are applied to correct for numerous systematic experimental effects. (F) Genetic interactions are measured by combining the corrected double mutant fitness and the fitnesses of the two single mutants. (G) Genetic interaction data is made available via the DRYGIN web database system.

Double mutant array plates are photographed in a light controlled environment using a high-resolution digital imaging system developed by S&P Robotics, Inc. (Toronto, ON). Digital images are processed using custom-developed image-processing software that measures colony area in terms of pixels (Tong *et al.*, 2004). Colony sizes are then stored in a PostgreSQL database for further manipulation and analysis. Thorough quality control procedures are applied to the data to ensure correct plate identity, screen quality, and proper image processing.

2.6. Quantitative scoring of genetic interactions using colony size-based fitness measurements

Quantitative genetic interactions define double mutant combinations that deviate from an expected phenotype (Bateson *et al.*, 1905). Mutations in independent genes often combine in a multiplicative manner and the resulting double mutant phenotype should be equivalent to the product of the two individual mutations (Mani *et al.*, 2008). The extent of the genetic interaction is consequently measured as $\varepsilon = f_{ab} - f_a f_b$, where f_a , f_b , and f_{ab} are quantitative fitness measures of the two single and the double mutant, respectively (Elena and Lenski, 1997). Negative genetic interactions ($\varepsilon < 0$) refer to double mutants showing a more severe fitness defect than expected, with the extreme case being synthetic lethality. Positive genetic interactions ($\varepsilon > 0$) refer to double mutants with a less severe fitness defect than expected and include interactions such as epistasis and suppression (Collins *et al.*, 2006; Mani *et al.*, 2008; Segre *et al.*, 2005).

To measure positive and negative genetic interactions quantitatively, precise estimates of both single and double mutant fitness are required. One method for measuring genetic interactions from yeast colony data derives single mutant fitness estimates from the average of all double mutants carrying the same query or array mutation (Collins *et al.*, 2006). Double mutant colony sizes are subsequently normalized by single mutant fitness and experimental variance estimates resulting in a single quantitative measure, termed S-score, which reflects both the strength and confidence of the genetic interaction (Collins *et al.*, 2006).

Although quantitative, the S-score does not represent a true fitness-based measure of genetic interaction. Furthermore, this approach does not account for several experimental effects associated with SGA technology that introduce strong systematic biases in large-scale genetic interaction datasets and are particularly pronounced for high-density arrays. These experimental artifacts adversely affect genetic interaction measurements resulting in increased false-positive rates and reduced sensitivity. Thus, we developed a novel method to process raw yeast colony sizes and derive true measures of fitness and genetic interaction (Baryshnikova *et al.*, manuscript in preparation).

To do so, we first identified several systematic experimental factors that contribute the vast majority of the observed variance in colony size and seriously interfered with our ability to detect and measure genetic interactions. Appropriate normalization of these experimental effects is critical to ensure accurate and reliable genetic interaction measurements. The systematic effects and normalization methods are summarized below and described in detail elsewhere (Baryshnikova *et al.*, manuscript in preparation).

Systematic effects and normalization procedures:

1. *Plate-specific effect correction*: normalizes differences in growth between plates due to varying incubation times and query single mutant fitness.
2. *Row/column effect correction*: normalizes differences in colony growth caused by differential exposure to nutrients due to plate position.
3. *Spatial effect correction*: normalizes differences in colony growth due to gradients in media thickness and/or relative proximity to heat sources.
4. *Competition effect correction*: normalizes differences in colony growth due to reduced fitness of neighboring mutant strains that results in reduced competition for nutrients.
5. *Batch effect normalization*: corrects for the striking similarity between genome-wide SGA screens conducted in parallel. We find that the set of screens completed by the same person, on the same robot and at the same time tend to share a common nonbiological signature. In other words, these screens share a set of unusually small or large colonies that could be confused with true genetic interactions, unless considered in the context of other screens performed in the same period of time.

To estimate double mutant fitness from colony size measurements we developed an approach that models colony size as a multiplicative combination of double mutant fitness, systematic experimental factors, and random noise. Specifically, for a double mutant deleted for genes a and b , we modeled colony size as $C_{ab} = f_{ab} \cdot s_{ab} \cdot e$, where C_{ab} is the colony area, f_{ab} is the double mutant fitness, s_{ab} is the combination of all systematic factors, and e is log-normally distributed error. In addition to double mutant fitness, we also obtained accurate single mutant fitness estimates (f_a and f_b) by averaging colony sizes for a given mutant across numerous control experiments using different arrays consisting of *kanMX4*- and *natMX4*-marked deletion mutants whose array positions have been randomized. Genetic interactions are subsequently measured by assuming the multiplicative model for independent genes, that is, $f_{ab} = f_a \cdot f_b + \varepsilon_{ab}$, where ε_{ab} represents the genetic interaction term between genes a and b (Baryshnikova *et al.*, manuscript in preparation).

Along with correcting for systematic effects and estimating the genetic interaction factor, we derived an accurate estimate of variance for the interaction. Our variance estimate is reported as a p -value that reflects both the local variability of replicate colonies (based on 4 colonies/plate

for each double mutant) and the variability of double mutants sharing the same query or array mutation.

Accounting for systematic effects and estimating genetic interactions and confidence levels separately provide a boost in data quality and capacity for predicting gene function from the resulting genetic interactions (Fig. 7.3). For example, functionally related genes are known to be enriched for genetic interactions and to share similar genetic interaction patterns. Using Gene Ontology coannotation as a measure of functional relatedness, genetic interactions measured using our newly developed score (SGA score) can predict 100 functionally related gene pairs with 62% precision (Fig. 7.3B, i). Failing to account for systematic experimental effects results in a significant reduction in precision (Fig. 7.3B, i). Analogously, similarity of genetic interaction profiles, as measured by Pearson correlation coefficients, computed using SGA scores predicts 100 functionally related gene pairs with 90% precision compared to only 15% precision when normalization procedures are not applied (Fig. 7.3B, ii).

Access to genetic interaction scores and confidence values is provided via a web database system (DRYGIN) which facilitates retrieval of interactions and their analysis (Koh *et al.*, 2010).

2.7. Interpretation and analysis of genetic interactions

Existing genetic interaction datasets in yeast have provided significant insight into the general principles of genetic network connectivity. For example, genes with related biological functions are connected by genetic interactions more often than expected by chance (Tong *et al.*, 2004) (Fig. 7.4). The position and the connectivity of the gene on the genetic interaction network is predictive of function. Moreover, because the genetic network is a small world network (Tong *et al.*, 2004), genes within the same neighborhood of the network tend to interact with one another and thus a sparsely mapped network is predictive of genetic interactions (Fig. 7.4B). Furthermore, synthetic lethal (negative) genetic interactions among nonessential genes generally do not correspond to physical interactions between the corresponding gene products. It has been observed that negative genetic interactions are more frequent between genes lying in different pathways, whereas physical interactions are more frequent among gene products functioning within the same pathway (Bader *et al.*, 2004; Collins *et al.*, 2007; Kelley and Ideker, 2005; Tong *et al.*, 2004; Ye *et al.*, 2005) (Fig. 7.4C). However, when a pathway or complex contain at least one essential gene, they are often enriched for so-called within-pathway synthetic lethal interactions, indicating that a subset of the negative genetic interactions for essential genes overlap with protein–protein interactions (Bandyopadhyay *et al.*, 2008; Boone *et al.*, 2007). Positive genetic interactions can connect members of the same protein complex or pathway. These positive within-pathway interactions may reflect that both the single and

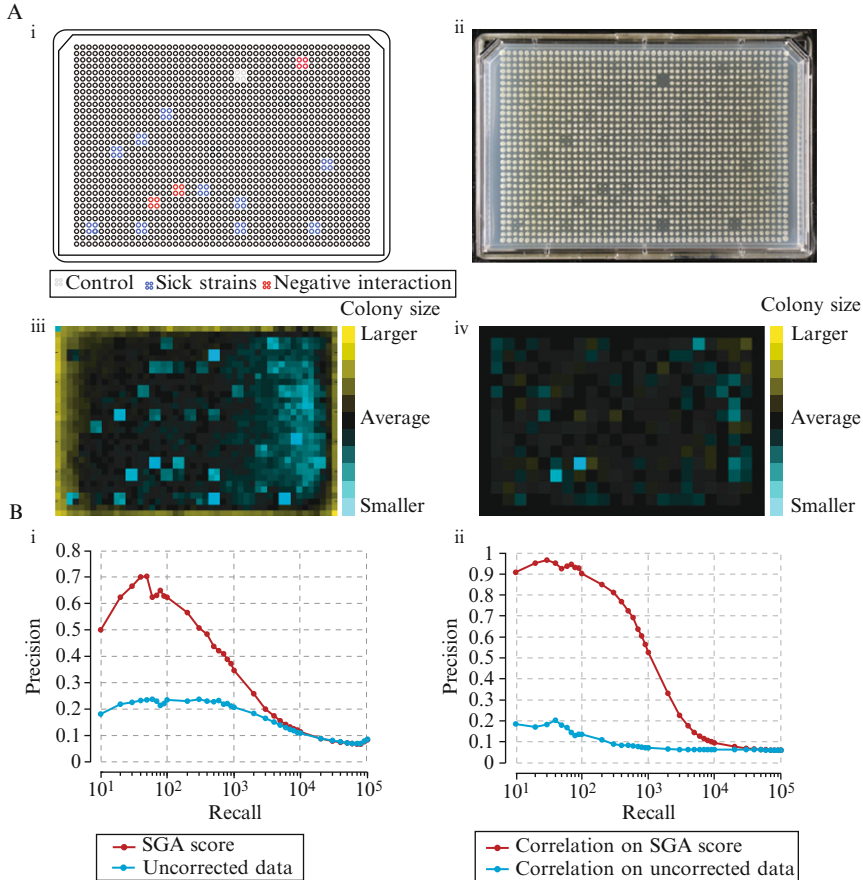


Figure 7.3 Systematic effect correction. (A) A schematic of a typical double mutant array plate shows the systematic biases affecting colony sizes. (i, ii) A typical double mutant array plate contains control spots (gray circles), strains with low fitness (blue circles), negative interactions (red circles), and positive interactions (not shown). On visual inspection, all three cases appear as small colonies or empty spots. (iii) Quantification of colony areas shows a distinctive spatial pattern affecting opposite sides of the plate (bigger colonies on the right, smaller colonies on the left) that was not obvious on visual inspection. Failure to correct for this spatial pattern will result in false-positive interactions. (iv) Corrects spatial patterns, eliminates false positives, and highlights true genetic interactions. (B) Precision–recall curves on genetic interaction scores (i) and genetic profile similarity (ii) show the increased functional prediction capacity of genetic data after correcting for systematic biases. A set of 1712 genome-wide SGA screens (Costanzo *et al.*, in press) were processed using the SGA score (Baryshnikova *et al.*, manuscript in preparation) and a version of the SGA score without systematic effect correction. Both direct genetic interactions and genetic profile similarities, as measured by Pearson correlations, were assessed for function by calculating precision and recall of functionally related gene pairs as described in the study of Myers *et al.* (2006). As a measure of functional relatedness, we used coannotation to the same Gene Ontology term.

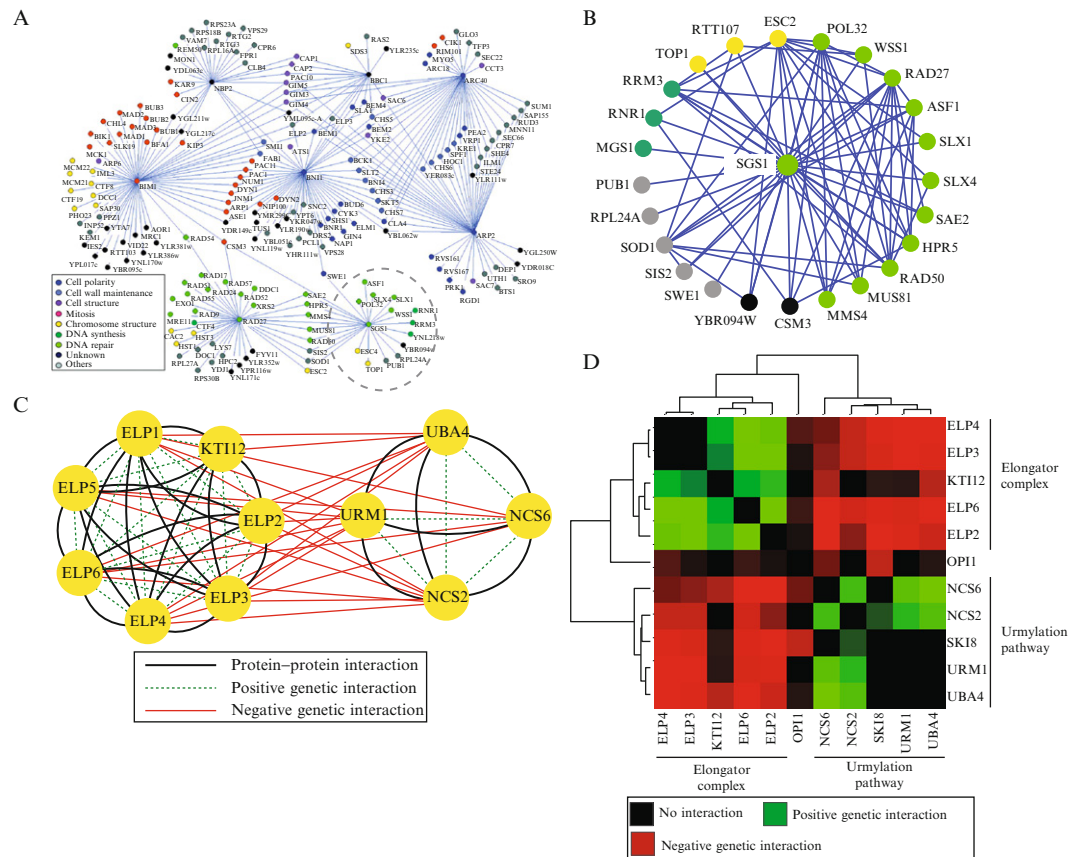
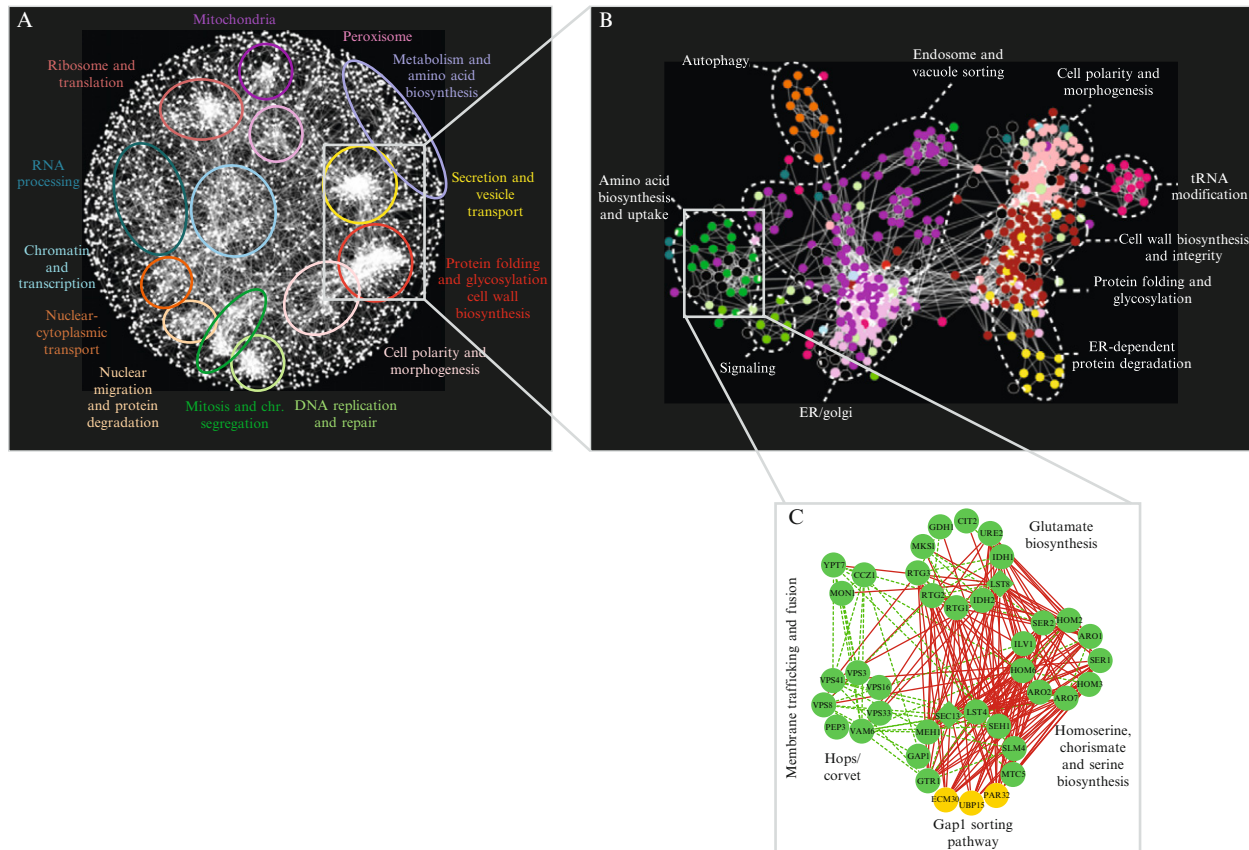


Figure 7.4 (Continued)

double mutants of nonessential linear pathways have the same fitness defect and therefore do not show the expected fitness defect associated with the multiplicative model. However, a more recent analysis of the global yeast physical interaction network as defined by affinity purification-mass spectrometry, yeast two-hybrid protocol, or protein-fragment complementation assay (PCA), showed that roughly an equivalent number of physical interactions overlap with negative and positive genetic interaction pairs: ~7% of protein-protein interacting pairs shared a negative genetic interaction, whereas ~5% shared a positive interaction (Costanzo *et al.*, in press). Conversely, only a small fraction of gene pairs that show a genetic interaction (0.4% negative and 0.5% positive) are also physically linked (Costanzo *et al.*, in press). These findings therefore suggest that the vast majority of both positive and negative interactions occurs between, rather than within, complexes and pathways, connecting those that presumably work together or buffer one another, respectively.

The synthetic lethal or negative genetic interaction profile for a particular query gene provides a rich phenotypic signature reflecting the function of the query as it contains genes involved in pathways that buffer the query. On average, negative interactions are approximately twofold more prevalent than positive interactions (Costanzo *et al.*, in press). However, we found subsets of genes that showed a strong bias in interaction type (up to 8–16-fold more negative than positive interactions or vice versa) (Costanzo *et al.*, in press). While the genetic interaction profile composed of negative genetic interactions carries more functional information than that composed only of positive interactions, the profile composed of both positive and negative interactions is most informative about gene function (Fig. 7.4). Clustering of genes according to their genetic interaction profiles is a simple yet very powerful tool for gene function prediction via a “guilt-by-association” approach (Figs. 7.4–7.5). Open source clustering software, such as Cluster 3.0 (<http://bonsai.ims.u-tokyo.ac.jp/~mdehoon/software/cluster/software.htm>), reassign rows

Figure 7.4 Properties of genetic interactions. (A) Example of a yeast synthetic lethal network. The synthetic lethal network is a sparse network, indicating that genetic interactions are rare. The frequency of true synthetic lethal interactions (blue lines) is less than 1%. A detailed description of how this initial network was generated can be found elsewhere (Tong *et al.*, 2001). (B) Functional neighborhood corresponding to indicated region (dashed gray circle) in (A). Despite being rare, synthetic lethal interactions (blue lines) occur frequently among genes that are functionally related, such as those involved in DNA replication and repair shown here. The frequency of synthetic lethal interaction between functionally related genes ranges from 18% to 25%. (C) Orthogonal relationships. Negative interactions tend to occur between nonessential complexes and pathways. Positive interactions overlap significantly with physical interactions and tend to connect members of the same pathway or complex. (D) Grouping genes according to patterns of genetic interactions revealed a functional relationship between the elongator complex and the urmylation pathway, which act in concert to modify specific tRNAs.



(query genes) and columns (array genes) of a genetic interaction matrix to place genes sharing similar genetic profiles next to each other. On the resulting clustergram, that is easily visualized with an open source application like Java Treeview (<http://jtreeview.sourceforge.net>), functionally related genes, including members of the same protein complex or pathway, are normally located in close proximity to each other and coclustering of genes of known function with poorly characterized genes provides strong evidence for cofunction (Tong *et al.*, 2004).

An alternative approach for clustering genetic interaction profiles consists in computing pair-wise correlation coefficients among all genes in a dataset (Costanzo *et al.*, in press; Kim *et al.*, 2001). The resulting data can be visualized as a network (using network visualization software such as Cytoscape (Shannon *et al.*, 2003)) where two genes are connected if their correlation exceeds a chosen threshold. The network can then be reorganized by a force-directed network layout in which highly correlated genes attract each other, while less correlated genes are repelled. Applying such an approach to the correlation-based genetic interaction network generates readily discernable clusters corresponding to distinct biological processes (Fig. 7.5A). This highly structured organization of the genetic map is maintained at increasing levels of resolution. For example, in one region of the global network, the related processes of endoplasmic reticulum

Figure 7.5 The genetic landscape of the cell. (A) A correlation-based network connecting genes with similar interaction profiles (Costanzo *et al.*, in press). Genetic profile similarities were measured for all gene pairs by computing Pearson correlation coefficients (PCC) from the complete genetic interaction matrix. Gene pairs whose profile similarity exceeded a PCC > 0.2 threshold were connected in the network. An edge-weighted, spring-embedded network layout, implemented in Cytoscape (Shannon *et al.*, 2003), was applied to determine node position based on genetic profile similarity. This resulted in the unbiased assembly of a network whereby genes sharing similar patterns of genetic interactions are proximal to each other in two-dimensional space, while less-similar genes are positioned further apart. Circled regions correspond to gene clusters enriched for the indicated biological processes. (B) Magnification of the functional map resolves cellular processes with increased specificity and enables precise functional predictions. A subnetwork corresponding to the indicated region of the global map is shown. Node color corresponds to a specific biological process; amino acid biosynthesis and uptake (dark green); signaling (light green); ER/Golgi (light purple); endosome and vacuole sorting (dark purple); ER-dependent protein degradation (yellow); protein glycosylation, cell wall biosynthesis and integrity (red); tRNA modification (fuchsia); cell polarity and morphogenesis (pink); autophagy (orange); uncharacterized (black). (C) Individual genetic interactions contributing to genetic profiles revealed by (B). A subset of genes belonging to the amino acid biosynthesis and uptake region of the network in (B). Nodes are grouped according to profile similarity and edges represent negative (red) and positive (green) genetic interactions. Nonessential (circles) and essential (diamonds) genes are colored according to the biological process indicated in (B) and uncharacterized genes are depicted in yellow.

(ER)/Golgi traffic, endosome/vacuole protein sorting, cell polarity, morphogenesis, cell wall integrity, protein folding, glycosylation, and ER-dependent protein degradation all cluster into well delineated groups (Fig. 7.5B). Furthermore, closer interrogation of the genetic map allows to distinguish uncharacterized genes located next to known functional clusters, suggesting previously unanticipated roles for the uncharacterized genes in the process (Fig. 7.5C).

2.8. *S. pombe* SGA

S. pombe or fission yeast is separated from *S. cerevisiae* by hundreds of millions of years of evolution and therefore provides an excellent system for exploring the conservation of genetic interactions. Moreover, *S. pombe* never underwent an ancient genome duplication and thus unlike *S. cerevisiae*, where functional complementation by paralogous genes can sometimes obscure genetic interactions, the corresponding *S. pombe* ortholog often shows a rich genetic interaction profile (Dixon and Boone, unpublished data). In addition, several gene classes and mechanisms are also absent in *S. cerevisiae* but present in *S. pombe* and other eukaryotes (Aravind *et al.*, 2000). For example, *S. pombe* has an RNA interference (RNAi) pathway similar to that seen in other eukaryotes, while baker's yeast does not (White and Allshire, 2008). Thus, analysis of genetic interactions in *S. pombe* should provide not only complementary information to that obtained in *S. cerevisiae*, but also insight into processes that are inaccessible in *S. cerevisiae*.

The sequencing of the *S. pombe* genome (Wood *et al.*, 2002) and subsequent availability of a genome-wide deletion collection from the commercial company Bioneer (<http://pombe.bioneer.co.kr/>) has driven the development of SGA-like techniques for this organism (Dixon *et al.*, 2008; Roguev *et al.*, 2007). For *S. pombe* SGA (SpSGA) (Dixon *et al.*, 2008), we developed a protocol that enabled efficient isolation of double mutant haploids through use of the high-density arraying capabilities of the Singer RoToR system.

A schematic illustrating the SpSGA procedure is shown in Fig. 7.6.

2.8.1. SpSGA procedure

Preparing the RoToR for use

1. Turn on the RoToR software and hardware and sterilize the interior using the integral UV lamp. From the main menu, select: LAMP and then set the timer for a minimum of 30 min.

Preparation of a 384-formatted query plate

1. Grow query strain in 8 ml YES liquid media, with shaking, overnight at 30 °C (or appropriate temperature for sensitive strains).

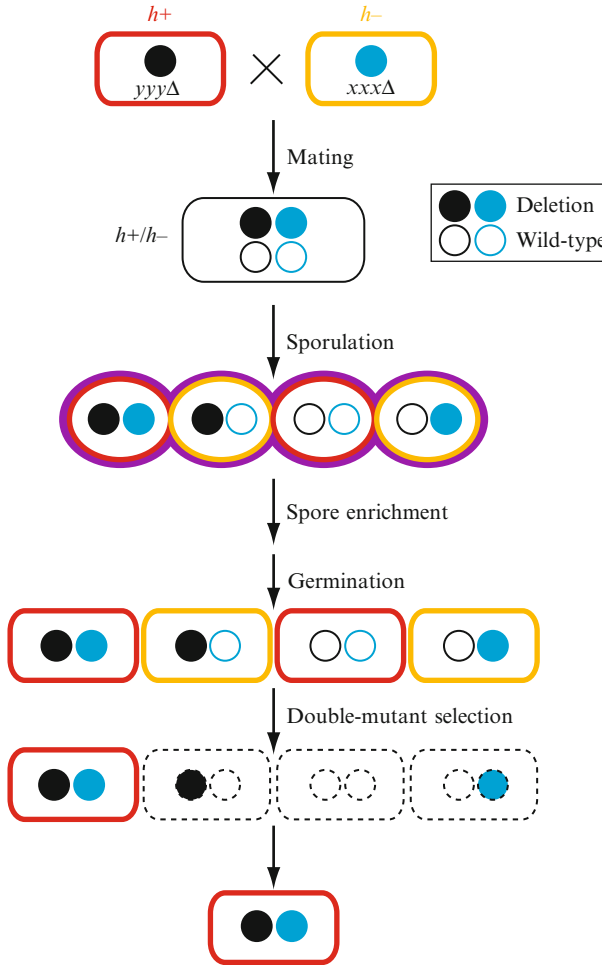


Figure 7.6 Outline of the SpSGA method. Cells of opposite mating type (h^+ , h^-) are mated on minimal SPA media and allowed to sporulate for 3 days at 26 °C. Then, to enrich for spores, mating plates are transferred to 42 °C for 3 days—a treatment that kills unmated haploid cells. Following spore enrichment, cells are transferred to rich medium to allow for germination, then transferred again to double-drug medium to select for recombinant double-mutant progeny. *S. pombe* haploids do not mate on rich medium; therefore, selection for a specific haploid mating type is not required.

2. Pour liquid culture into an empty PlusPlate dish, ensuring the entire surface area is covered.
3. Place the source dish containing the liquid culture in the black position. Place the YES (agar) target plate in the red position. With the RoToR, select: LIQUID HANDLING → BATH → BATH-96. As prompted, load the hopper with 96 long pin pads. Under OPTIONS check

ECONOMY and REVISIT SOURCE. Start the program. This will transfer a droplet of the culture to each position on the array in four steps, generating a 384 array (4×96). *Caution.* When in use, the RoToR robot arm and turntable move very quickly. Ensure that the safety cover is in place during operation and that hands and loose clothing are kept well free of the moving parts.

4. Grow the query plate in an incubator at 30 °C for 2 days or until sufficient growth is obtained. With larger colonies, a single query plate can be used for multiple matings.

Preparation of a 384-formatted array plate

1. Plates obtained from Bioneer are arrayed in a 96-position format. These can be rearranged 1:4, giving four copies of each query or rearranged at higher density (possibly could use the RoToR 4→1 arraying protocol, although we have not tried that ourselves).
2. Grow the array plate in an incubator at 30 °C for 2 days or until sufficient growth is obtained.

Mating of query to array

1. Place the YES query source plate in the blue position, the YES array source plate in the red position, and the target SPA mating plate in the black position. With the RoToR, select: MATE → 384. Load the hopper with the appropriate number of 384 short pin pads. Start the program.
2. Remove the SPA mating dish and set aside for further processing. The query and/or array source dishes can continue to be used as needed. *Critical step.* It is essential that the query and array source plates are freshly grown (typically 2 days growth is optimal). Plates used after storage at 4 °C do not mate as efficiently. Depending on the amount of cell growth, a single 384-format query plate can be mated to 3–4 separate array plates. However, further attempts may result in a reduced number of transferred cells, interfering with mating efficiency.
3. Following the transfer of cells onto the SPA plate, use the RoToR to transfer a drop of sterile H₂O onto the mated cells and mix them together. Load a PlusPlate dish containing sterile H₂O into the black position and a freshly mated SPA plate in the red position. On the RoToR select: LIQUID HANDLING → BATH → BATH-96. Load 96 long pin pads. Under advanced options, select the Agar Mix tab and set a mix diameter of 0.2 mm. Start the program. *Critical step.* A droplet of water together with the punching of the agar is thought to facilitate access of each yeast to the other. This greatly enhances the mating efficiency, compared to no mixing conditions, and thereby

enhances sporulation substantially. This in turn reduces the number of unmated haploids that need to be eliminated in subsequent steps.

4. Put SPA plates at 26 °C and allow cells to proceed through conjugation and sporulation for 3 days.
5. Put SPA dishes at 42 °C for 3 days. *Critical step.* Ensure that the incubator is maintained at 42 °C. Higher or lower temperatures are not as efficient at eliminating unmated haploids. *Note:* significant temperature gradients may be observed within certain incubators, so it is advisable to measure the temperature at several places within the enclosure.
6. Transfer spores to YES plates as follows. Load the SPA source plate into the red position and the YES target plate into the blue position. Using the RoToR, select: AGAR-AGAR → REPLICATE → REPLICATE ONE → 384-1536. Load the hopper with 384 short pin pads and start the program using default advanced options with “revisit source” enabled.
7. *Pause point.* Once spores have been transferred to YES plates, it is advisable to store the SPA mating plates at 4 °C. Spores remaining on this plate can be subsequently stored up to several months and used later as a source of spores for further confirmatory experiments, such as random spore analysis.
8. Put YES plates at 30 °C and allow cells to germinate for at least 2 days.
9. Transfer germinated cells from source YES plates loaded in the red position to YES + G418 + Nat target plates loaded in the blue position. With the RoToR, select: AGAR-AGAR → REPLICATE → REPLICATE ONE → 1536-1536. Load the hopper with 1536 short pin pads and start the program using default advanced options.
10. Transfer YES + G418 + Nat plates to 30 °C to allow cells to grow for 2 days.
11. *Pause point.* Once yeast cells have grown up on YES + G418 + Nat plates they can be further processed right away, or stored at 4 °C for up to several months for subsequent processing.
12. Image plates to acquire colony size measurements or carry on with additional analysis of recombinant haploids.

3. MEDIA AND STOCK SOLUTIONS

3.1. SGA media and stock solutions

1. *G418 (Geneticin, Invitrogen)*: Dissolve in water at 200 mg/ml, filter sterilize, and store in aliquots at 4 °C.
2. *clonNAT (nourseothricin, Werner BioAgents, Jena, Germany)*: Dissolve in water at 100 mg/ml, filter sterilize, and store in aliquots at 4 °C.

3. *Canavanine* (*L-canavanine sulfate salt*, Sigma, C-9758): Dissolve in water at 100 mg/ml, filter sterilize, and store in aliquots at 4 °C.
4. *Thialysine* (*S*-(2-aminoethyl)-*L*-cysteine hydrochloride, Sigma, A-2636): Dissolve in water at 100 mg/ml, filter sterilize, and store in aliquots at 4 °C.
5. *Amino acids supplement powder mixture for synthetic media (complete)*: Contains 3 g adenine (Sigma), 2 g uracil (ICN), 2 g inositol, 0.2 g para-aminobenzoic acid (Acros Organics), 2 g alanine, 2 g arginine, 2 g asparagine, 2 g aspartic acid, 2 g cysteine, 2 g glutamic acid, 2 g glutamine, 2 g glycine, 2 g histidine, 2 g isoleucine, 10 g leucine, 2 g lysine, 2 g methionine, 2 g phenylalanine, 2 g proline, 2 g serine, 2 g threonine, 2 g tryptophan, 2 g tyrosine, and 2 g valine (Fisher). Drop-out (DO) powder mixture is a combination of the above ingredients minus the appropriate supplement. Two grams of the DO powder mixture is used per liter of medium.
6. *Amino acids supplement for sporulation medium*: Contains 2 g histidine, 10 g leucine, 2 g lysine, 2 g uracil; 0.1 g of the amino acid supplements powder mixture is used per liter of sporulation medium.
7. *Glucose* (*Dextrose*, Fisher): Prepare 40% solution, autoclave, and store at room temperature.
8. *YEPD*: Add 120 mg adenine (Sigma), 10 g yeast extract, 20 g peptone, 20 g bacto agar (BD Difco) to 950 ml water in a 2 l flask. After autoclaving, add 50 ml of 40% glucose solution, mix thoroughly, cool to ~65 °C and pour plates.
9. *YEPD + G418*: Cool YEPD medium to ~65 °C, add 1 ml of G418 stock solution (final concentration 200 mg/l), mix thoroughly, and pour plates.
10. *YEPD + clonNAT*: Cool YEPD medium to ~65 °C, add 1 ml of clonNAT stock solution (final concentration 100 mg/l), mix thoroughly, and pour plates.
11. *YEPD + G418/clonNAT*: Cool YEPD medium to ~65 °C, add 1 ml of G418 (final concentration 200 mg/l), and 1 ml of clonNAT (final concentration 100 mg/l) stock solutions, mix thoroughly, and pour plates.
12. *Enriched sporulation*: Add 10 g potassium acetate (Fisher), 1 g yeast extract, 0.5 g glucose, 0.1 g amino acids supplement powder mixture for sporulation, 20 g bacto agar to 1 l water in a 2 l flask. After autoclaving, cool medium to ~65 °C, add 250 µl of G418 stock solution (final concentration 50 mg/l), mix thoroughly, and pour plates.
13. *(SD/MSG) – His/Arg/Lys + canavanine/thialysine/G418*: Add 1.7 g yeast nitrogen base w/o amino acids or ammonium sulfate (BD Difco), 1 g MSG (L-glutamic acid sodium salt hydrate, Sigma), 2 g amino acids supplement powder mixture (DO – His/Arg/Lys), 100 ml water in a 250 ml flask. Add 20 g bacto agar to 850 ml water in a 2 l flask. Autoclave separately. Combine autoclaved solutions, add 50 ml 40%

glucose, cool medium to $\sim 65^{\circ}\text{C}$, add 0.5 ml canavanine (50 mg/l), 0.5 ml thialysine (50 mg/l), and 1 ml G418 (200 mg/l) stock solutions, mix thoroughly, and pour plates. Ammonium sulfate impedes the function of G418 and clonNAT. Hence, synthetic medium containing these antibiotics is made with monosodium glutamic acid as a nitrogen source (Cheng *et al.*, 2000).

14. (SD/MSG) – His/Arg/Lys + canavanine/thialysine/clonNAT: Add 1.7 g yeast nitrogen base w/o amino acids or ammonium sulfate, 1 g MSG, 2 g amino acids supplement powder mixture (DO – His/Arg/Lys), 100 ml water in a 250 ml flask. Add 20 g bacto agar to 850 ml water in a 2 l flask. Autoclave separately. Combine autoclaved solutions, add 50 ml 40% glucose, cool medium to $\sim 65^{\circ}\text{C}$, add 0.5 ml canavanine (50 mg/l), 0.5 ml thialysine (50 mg/l), and 1 ml clonNAT (100 mg/l) stock solutions, mix thoroughly, and pour plates.
15. (SD/MSG) – His/Arg/Lys + canavanine/thialysine/G418/clonNAT: Add 1.7 g yeast nitrogen base w/o amino acids or ammonium sulfate, 1 g MSG, 2 g amino acids supplement powder mixture (DO – His/Arg/Lys), 100 ml water in a 250 ml flask. Add 20 g bacto agar to 850 ml water in a 2 l flask. Autoclave separately. Combine autoclaved solutions, add 50 ml 40% glucose, cool medium to $\sim 65^{\circ}\text{C}$, add 0.5 ml Canavanine (50 mg/l), 0.5 ml thialysine (50 mg/l), 1 ml G418 (200 mg/l) and 1 ml clonNAT (100 mg/l) stock solutions, mix thoroughly, and pour plates.
16. (SD/MSG) Complete: Add 1.7 g yeast nitrogen base w/o amino acids or ammonium sulfate, 1 g MSG, 2 g amino acids supplement powder mixture (complete), 100 ml water in a 250 ml flask. Add 20 g bacto agar to 850 ml water in a 2 l flask. Autoclave separately. Combine autoclaved solutions, add 50 ml of 40% glucose, mix thoroughly, cool medium to $\sim 65^{\circ}\text{C}$ and pour plates.
17. SD – His/Arg/Lys + canavanine/thialysine: Add 6.7 g yeast nitrogen base w/o amino acids (BD Difco), 2 g amino acids supplement powder mixture (DO – His/Arg/Lys), 100 ml water in a 250 ml flask. Add 20 g bacto agar to 850 ml water in a 2 l flask. Autoclave separately. Combine autoclaved solutions, add 50 ml 40% glucose, cool medium to $\sim 65^{\circ}\text{C}$, add 0.5 ml canavanine (50 mg/l) and 0.5 ml thialysine (50 mg/l) stock solutions, mix thoroughly, and pour plates. This medium does not contain any antibiotics such as G418 or clonNAT and therefore ammonium sulfate is used as the nitrogen source.
18. SD – Leu/Arg/Lys + canavanine/thialysine: Add 6.7 g yeast nitrogen base w/o amino acids, 2 g amino acids supplement powder mixture (DO – Leu/Arg/Lys), 100 ml water in a 250 ml flask. Add 20 g bacto agar to 850 ml water in a 2 l flask. Autoclave separately. Combine autoclaved solutions, add 50 ml 40% glucose, cool medium to $\sim 65^{\circ}\text{C}$, add 0.5 ml canavanine (50 mg/l) and 0.5 ml thialysine (50 mg/l) stock solutions, mix thoroughly, and pour plates.

3.2. SpSGA media and stock solutions

1. *250 mg/ml of G418 solution*. Dissolve 2.5 g G418 in 10 ml of water. Filter sterilize with a 0.22 μm screw cap filter.
2. *100 mg/ml of clonNat solution*. Dissolve 1 g clonNat in 10 ml of water. Filter sterilize with a 0.22 μm screw cap filter.
3. *SPA-agar plates (SPA plates)*. Add 30 g agar, 10 g dextrose, 1 g of KH_2PO_4 , and 1 ml of 1000 \times vitamin stock to 1 l of water. Autoclave and then pour 50 ml per PlusPlate dish. Allow to solidify and either use right away or store at 4 $^\circ\text{C}$ until needed.
4. *1000 \times vitamin stock*. Dissolve 1 g pantothenic acid, 10 g nicotinic acid, 10 g inositol, and 10 mg biotin in 1 l of water.
5. *YES media and plates*. Add 30 g glucose, 5 g yeast extract, 225 mg adenine, 225 mg L-histidine, 225 mg leucine, 225 mg uracil, and 225 mg lysine to 1 l of water. Autoclave and then cool to 55 $^\circ\text{C}$ before adding appropriate antibiotics (1:1000 dilution). To make solid media, add 30 g agar prior to autoclaving and pour 50 ml per PlusPlate.

4. APPLICATIONS OF SGA METHODOLOGY

Most large-scale studies have focused on fitness as the primary phenotype to identify genetic interactions (St Onge *et al.*, 2007; Tong *et al.*, 2004). In theory, all phenotypes are measurable and amenable to genetic interaction analyses. SGA methodology provides an efficient and systematic means for combining mutations and can be readily applied to identify additional genetic interactions that do not result in overt fitness defects. For example, reporter-gene constructs can be incorporated into the SGA methodology to monitor specific transcriptional responses in the ~ 5000 deletion mutant backgrounds (Costanzo *et al.*, 2004; Fillingham *et al.*, 2009) and used as an alternative to fitness for uncovering genetic interactions (Jonikas *et al.*, 2009). Integrating SGA technology with methodologies for measuring a diverse set of phenotypes generates networks that provide comprehensive genome coverage and accurately reflect global cellular functions.

4.1. Integrating SGA and high-content screening

Combining SGA technology with different cytological reporters and high content screening (HCS) methodologies also enables identification of mutant combinations that lack obvious growth defects but elicit subtle yet unexpected cell biological phenotypes (Vizeacoumar *et al.*, 2009, 2010). A HCS platform gathers cell biological information for genome-wide arrays of mutants by first acquiring cell images and then quantifying specific morphological phenotypes

following image processing (Fig. 7.7). The following section describes the steps involved in this procedure and can be applied to monitor virtually any subcellular event within the cell. The media required for various selections are described in detail in Section 3.

1. Cross the SGA query strain expressing the cell biological reporter to the deletion array as described in Section 2.4.
2. Once the *MATa-kanMX4* meiotic progeny is selected on agar plates as described in Section 2.4, transfer the cultures to liquid. Select for *MATa-kanMX4-natMX4* meiotic progeny by inoculating the cells in (SD/MSG) – His/Arg/Lys + canavanine/thialysine/G418/clonNAT liquid media in 96-well format plates. Note to include the auxotrophic selection of the reporter throughout the process.
3. Grow liquid cultures overnight at the desired temperature in 96-well plates containing 3 mm glass beads (Fisher Scientific). Seal the plates with breathable adhesive membranes (Corning).
4. Dispense appropriate volume of samples based on the optical density of each sample to 96-well filter plates (Whatmann) using a liquid handling robot (Biomek FX), to ensure uniform and optimal cell densities for subsequent image analysis.
5. Vacuum the filter plates (NucleoVac96 vacuum manifold, Macherey-Nagel) and wash the cells in sterile distilled water using plate washer (Multidrop384 Liquid Dispenser System, Thermo Electron Corporation). Vacuum the plates again so that only the washed cells remain in the filter plates.
6. Add low-fluorescence medium (Sheff and Thorn, 2004) with appropriate drug selection to the filter plates to resuspend the washed cells and transfer cells from the filter plates to 96-well optical plates (Matrical), using the liquid handler (Biomek FX) and let the cells settle down. Seal the plates with aluminum foil (VWR) to prevent drying of the samples.
7. Load the plates into an automated incubator (Cytomat, Thermo Fisher Scientific, Inc.) and store the plates at 4 °C prior to imaging to avoid over growth. Automate the platform such that each plate is incubated at 30 °C for 30–45 min prior to imaging. Using a robotic arm (CRS Catalyst Express, Thermo Electron Corporation) transfer the plates to the wide-field HCS imager (ImageXpress5000A, MDS Analytical, Inc.).
8. Image plates using a 60× air-objective collecting at least 4–6 images per well averaging to as many as 200 cells per mutant. Ensure proper storage of images in a database to readily access them for automated image analysis.
9. Analyze the images using an image-analysis software with throughput capabilities (MetaXpress software v1.6, MDS Analytical, Inc.) and extract morphometric features to generate a unique profile for each mutant. Open source software developed by academic labs, such as

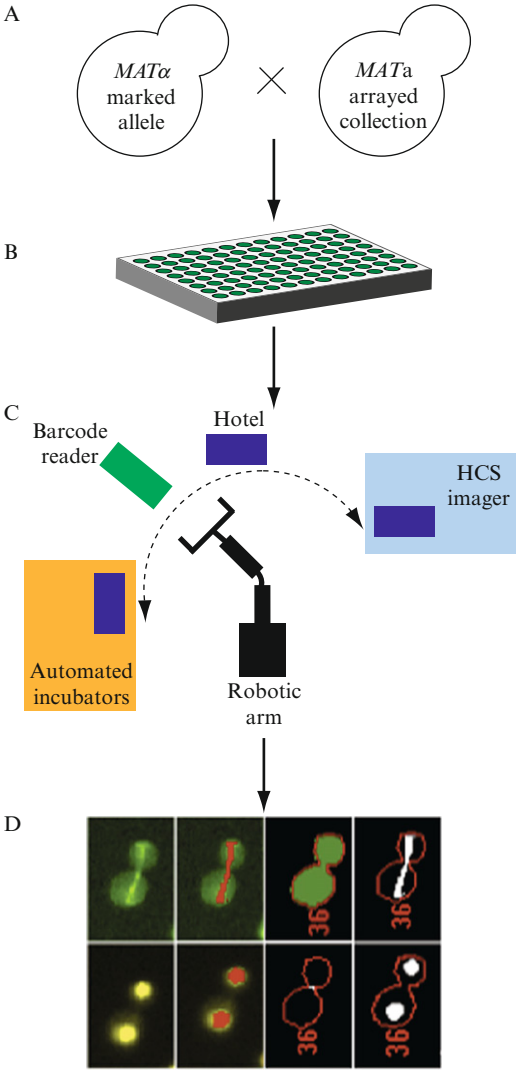


Figure 7.7 SGA-HCS pipeline for evaluation of cell biological phenotypes. (A) Using the SGA methodology, a fluorescent marker can be introduced into the arrayed deletion collection. (B) Deletion mutant colonies expressing a fluorescent marker are transferred to optical plates containing liquid selection media for imaging. (C) A robotic arm is used to move optical plates between incubators and the HCS imaging system. (D) Automated image analysis software, such as MetaXpress, is used to detect fluorescent signal and measure morphological features.

CellProfiler, may also be used for this purpose (Carpenter, 2007). Briefly, after shade correction and background subtraction, apply a segmentation technique such as thresholding, so that the range of signal intensity that pertains to cellular objects is selected separating bright cellular objects from the dark image background. Following object identification, quantitative measurements of each cell can be used to extract numerous morphometric parameters, a feature available in most image-analysis software.

Statistical analysis and data mining for multiplexed high content analysis (HCA) is still in its infancy. Hence, most HCA are custom designed and also require manual inspection of images (Bakal *et al.*, 2007; Corcoran *et al.*, 2004; Eggert *et al.*, 2004; Gururaja *et al.*, 2006; Loo *et al.*, 2007; Narayanaswamy *et al.*, 2006; Tanaka *et al.*, 2005). However, a more straightforward approach is to compare each mutant population read out against that of the wild-type cell population, and identify statistically deviant mutants for any desired feature. Methods to standardize HCA are still in progress and the continued development of these procedures to process HCS data without sacrificing information accuracy will be of paramount significance.

4.2. Essential gene and higher order genetic interactions

This chapter focuses on the application of SGA analysis to generate double mutant strains and identify genetic interactions among nonessential deletion mutants. However, SGA can also be applied to examine synthetic genetic interactions involving essential genes. For example, an SGA query strain can be crossed to the Tet-promoter collection (yTHC, Open Biosystems), double mutants can be selected and scored for growth defects in the presence of doxycycline, which downregulates the expression of the essential genes (Davierwala *et al.*, 2005). Other essential gene mutant collections (Ben-Aroya *et al.*, 2008; Schuldiner *et al.*, 2005) are now available in arrayed formats and are amenable to genetic interaction analyses using SGA technology (Costanzo *et al.*, in press).

While digenic interactions are more commonly studied, SGA methodology can be easily applied to examine higher order genetic interactions involving more than two genes (Tong *et al.*, 2004).

4.3. Combining SGA and gene overexpression libraries

In addition to loss-of-function mutations, SGA can be easily adapted to examine different forms of genetic interactions involving high-copy plasmid or regulatory expression of yeast or heterologous genes. Several gene overexpression libraries have been constructed, in recent years (Gelperin *et al.*, 2005; Hu *et al.*, 2007; Jones *et al.*, 2008; Zhu *et al.*, 2001). One of these

libraries was used to assemble a Yeast Overexpression Array, containing ~6000 ORFs (Yeast GST-Tagged Collection, Open Biosystems), and was combined with SGA to screen for synthetic dosage lethality and suppression (Sopko *et al.*, 2006). This proved to be a successful strategy for identifying downstream targets regulated by specific signaling pathways (Sopko *et al.*, 2006, 2007). The development of new plasmid libraries carrying genes under inducible expression will expand the potential for dosage lethality (Gelperin *et al.*, 2005; Hu *et al.*, 2007), whereas the development of libraries in which each gene is under the control of its own promoter (Ho *et al.*, 2009; Jones *et al.*, 2008) offers the potential for building other overexpression arrays that may be particularly useful for dosage suppression experiments.

4.4. Applying SGA as a method for high-resolution genetic mapping (SGAM)

Because double mutants are created by meiotic recombination, a set of gene deletions that is linked to the query gene, which we refer to as the “linkage group” form double mutants at a reduced frequency, thus, appearing synthetic lethal/sick with the query mutation. Since the gene deletions represent mapping markers covering all chromosomes in the yeast genome, SGA mapping (SGAM) has been shown as an effective method for high-resolution genetic mapping (Chang *et al.*, 2005; Jorgensen *et al.*, 2002). In addition to mapping of recessive alleles, SGAM is particularly useful for rapid mapping of dominant mutations, which are challenging to clone using standard techniques (Menne *et al.*, 2007).

4.5. Chemical genomics

Because chemical perturbations mimic genetic perturbations, genetic networks also provide a key for predicting the targets of inhibitory bioactive molecules (Parsons *et al.*, 2004) (Fig. 7.8). If a compound inhibits a specific target protein, then the chemical-genetic profile, the set of mutants that are hypersensitive to the compound, should overlap with the genetic interaction profile of the target gene. As a result, the compound and its target should cocluster together and with other genes and compounds involved in the same biological process (Fig. 7.8).

The integration of ~1700 genetic interaction profiles with ~400 drug sensitivity profiles (Costanzo *et al.*, in press) proved that compounds with known functions, such as hydroxyurea, which inhibits DNA synthesis, or tunicamycin, which inhibits glycosylation, cluster to their expected biological process (Giaever *et al.*, 1999). Furthermore, the target of a novel drug, now named Erodoxin, was identified via inspection of a combined chemical-genetic correlation network. Thus, this chemical-genetic approach to

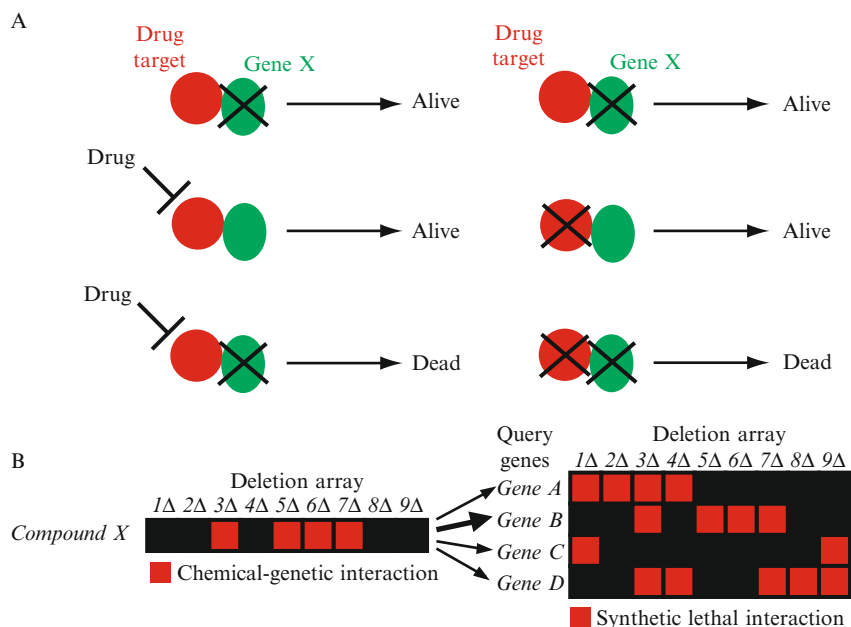


Figure 7.8 Chemical-genetic interactions can be modeled by synthetic genetic interactions. (A) In a chemical-genetic interaction (at left), a deletion mutant, lacking the product of the deleted gene (represented by a black X), is hypersensitive to a normally sublethal concentration of a growth-inhibitory compound. In a synthetic lethal genetic interaction (right), two single deletions lead to viable mutants but are inviable in a double-mutant combination. Gene deletion alleles that show chemical-genetic interactions with a particular compound should also be synthetically lethal or sick with a mutation in the compound target gene. (B) Comparison of a chemical-genetic profile to a compendium of genetic interaction (synthetic lethal) profiles should identify the pathways and targets inhibited by drug treatment. In this hypothetical figure, chemical-genetic and genetic interactions are both designated by red squares. For example, deletion mutants 3, 5, 6, and 7 are hypersensitive to compound X and a mutation in query gene A leads to a fitness defect when combined with deletion alleles 1, 2, 3, and 4. Here, the chemical-genetic profile of compound X resembles the genetic profile of gene B, thereby identifying the product of gene B as a putative target of compound X.

mode-of-action analysis complements haploinsufficiency profiling, which focuses on identifying the drug target directly (Giaever *et al.*, 1999; Hillenmeyer *et al.*, 2008).

REFERENCES

- Aravind, L., *et al.* (2000). Lineage-specific loss and divergence of functionally linked genes in eukaryotes. *Proc. Natl. Acad. Sci. USA* **97**, 11319–11324.
- Bader, J. S., *et al.* (2004). Gaining confidence in high-throughput protein interaction networks. *Nat. Biotechnol.* **22**, 78–85.

- Bakal, C., *et al.* (2007). Quantitative morphological signatures define local signaling networks regulating cell morphology. *Science* **316**, 1753–1756.
- Bandyopadhyay, S., *et al.* (2008). Functional maps of protein complexes from quantitative genetic interaction data. *PLoS Comput. Biol.* **4**, e1000065.
- Bateson, W., *et al.* (1905). Reports to the Evolution Committee of the Royal Society. Report II. Harrison and Sons, London.
- Ben-Aroya, S., *et al.* (2008). Toward a comprehensive temperature-sensitive mutant repository of the essential genes of *Saccharomyces cerevisiae*. *Mol. Cell* **30**, 248–258.
- Boone, C., *et al.* (2007). Exploring genetic interactions and networks with yeast. *Nat. Rev. Genet.* **8**, 437–449.
- Carpenter, A. E. (2007). Image-based chemical screening. *Nat. Chem. Biol.* **3**, 461–465.
- Chang, M., *et al.* (2005). RMI1/NCE4, a suppressor of genome instability, encodes a member of the RecQ helicase/Topo III complex. *EMBO J.* **24**, 2024–2033.
- Cheng, T. H., *et al.* (2000). Controlling gene expression in yeast by inducible site-specific recombination. *Nucleic Acids Res.* **28**, E108.
- Collins, S. R., *et al.* (2006). A strategy for extracting and analyzing large-scale quantitative epistatic interaction data. *Genome Biol.* **7**, R63.
- Collins, S. R., *et al.* (2007). Functional dissection of protein complexes involved in yeast chromosome biology using a genetic interaction map. *Nature* **446**, 806–810.
- Corcoran, L. J., *et al.* (2004). A novel action of histone deacetylase inhibitors in a protein aggresome disease model. *Curr. Biol.* **14**, 488–492.
- Costanzo, M., *et al.* (2004). CDK activity antagonizes Whi5, an inhibitor of G1/S transcription in yeast. *Cell* **117**, 899–913.
- Davierwala, A. P., *et al.* (2005). The synthetic genetic interaction spectrum of essential genes. *Nat. Genet.* **37**, 1147–1152.
- Decourty, L., *et al.* (2008). Linking functionally related genes by sensitive and quantitative characterization of genetic interaction profiles. *Proc. Natl. Acad. Sci. USA* **105**, 5821–5826.
- Dixon, S. J., *et al.* (2008). Significant conservation of synthetic lethal genetic interaction networks between distantly related eukaryotes. *Proc. Natl. Acad. Sci. USA* **105**, 16653–16658.
- Dixon, S. J., *et al.* (2009). Systematic mapping of genetic interaction networks. *Annu. Rev. Genet.* **43**, 601–625.
- Eggert, U. S., *et al.* (2004). Parallel chemical genetic and genome-wide RNAi screens identify cytokinesis inhibitors and targets. *PLoS Biol.* **2**, e379.
- Elena, S. F., and Lenski, R. E. (1997). Test of synergistic interactions among deleterious mutations in bacteria. *Nature* **390**, 395–398.
- Fay, D. S., *et al.* (2002). *fzr-1* and *lin-35/Rb* function redundantly to control cell proliferation in *C. elegans* as revealed by a nonbiased synthetic screen. *Genes Dev.* **16**, 503–517.
- Fillingham, J., *et al.* (2009). Two-color cell array screen reveals interdependent roles for histone chaperones and a chromatin boundary regulator in histone gene repression. *Mol. Cell* **35**, 340–351.
- Gelperin, D. M., *et al.* (2005). Biochemical and genetic analysis of the yeast proteome with a movable ORF collection. *Genes Dev.* **19**, 2816–2826.
- Giaever, G., *et al.* (1999). Genomic profiling of drug sensitivities via induced haploinsufficiency. *Nat. Genet.* **21**, 278–283.
- Giaever, G., *et al.* (2002). Functional profiling of the *Saccharomyces cerevisiae* genome. *Nature* **418**, 387–391.
- Goldstein, A. L., and McCusker, J. H. (1999). Three new dominant drug resistance cassettes for gene disruption in *Saccharomyces cerevisiae*. *Yeast* **15**, 1541–1553.
- Gururaja, T. L., *et al.* (2006). R-253 disrupts microtubule networks in multiple tumor cell lines. *Clin. Cancer Res.* **12**, 3831–3842.

- Hartman, J. L., *et al.* (2001). Principles for the buffering of genetic variation. *Science* **291**, 1001–1004.
- Hillenmeyer, M. E., *et al.* (2008). The chemical genomic portrait of yeast: Uncovering a phenotype for all genes. *Science* **320**, 362–365.
- Ho, C. H., *et al.* (2009). A molecular barcoded yeast ORF library enables mode-of-action analysis of bioactive compounds. *Nat. Biotechnol.* **27**, 369–377.
- Hu, Y., *et al.* (2007). Approaching a complete repository of sequence-verified protein-encoding clones for *Saccharomyces cerevisiae*. *Genome Res.* **17**, 536–543.
- Jones, G. M., *et al.* (2008). A systematic library for comprehensive overexpression screens in *Saccharomyces cerevisiae*. *Nat. Methods* **5**, 239–241.
- Jonikas, M. C., *et al.* (2009). Comprehensive characterization of genes required for protein folding in the endoplasmic reticulum. *Science* **323**, 1693–1697.
- Jorgensen, P., *et al.* (2002). High-resolution genetic mapping with ordered arrays of *Saccharomyces cerevisiae* deletion mutants. *Genetics* **162**, 1091–1099.
- Kelley, R., and Ideker, T. (2005). Systematic interpretation of genetic interactions using protein networks. *Nat. Biotechnol.* **23**, 561–566.
- Kim, S. K., *et al.* (2001). A gene expression map for *Caenorhabditis elegans*. *Science* **293**, 2087–2092.
- Koh, *et al.* (2010). *Nucleic Acids Res.* **38**, D502–D507.
- Levy, S., *et al.* (2007). The diploid genome sequence of an individual human. *PLoS Biol.* **5**, e254.
- Loo, L. H., *et al.* (2007). Image-based multivariate profiling of drug responses from single cells. *Nat. Methods* **4**, 445–453.
- Lucchesi, J. C. (1968). Synthetic lethality and semi-lethality among functionally related mutants of *Drosophila melanogaster*. *Genetics* **59**, 37–44.
- Mani, R., *et al.* (2008). Defining genetic interaction. *Proc. Natl. Acad. Sci. USA* **105**, 3461–3466.
- Menne, T. F., *et al.* (2007). The Shwachman–Bodian–Diamond syndrome protein mediates translational activation of ribosomes in yeast. *Nat. Genet.* **39**, 486–495.
- Mnaimneh, S., *et al.* (2004). Exploration of essential gene functions via titratable promoter alleles. *Cell* **118**, 31–44.
- Myers, C. L., *et al.* (2006). Finding function: Evaluation methods for functional genomic data. *BMC Genomics* **7**, 187.
- Narayanawamy, R., *et al.* (2006). Systematic profiling of cellular phenotypes with spotted cell microarrays reveals mating-pheromone response genes. *Genome Biol.* **7**, R6.
- Pan, X., *et al.* (2004). A robust toolkit for functional profiling of the yeast genome. *Mol. Cell* **16**, 487–496.
- Pan, X., *et al.* (2006). A DNA integrity network in the yeast *Saccharomyces cerevisiae*. *Cell* **124**, 1069–1081.
- Parsons, A. B., *et al.* (2004). Integration of chemical-genetic and genetic interaction data links bioactive compounds to cellular target pathways. *Nat. Biotechnol.* **22**, 62–69.
- Roguev, A., *et al.* (2007). High-throughput genetic interaction mapping in the fission yeast *Schizosaccharomyces pombe*. *Nat. Methods* **4**, 861–866.
- Schuldiner, M., *et al.* (2005). Exploration of the function and organization of the yeast early secretory pathway through an epistatic miniarray profile. *Cell* **123**, 507–519.
- Segre, D., *et al.* (2005). Modular epistasis in yeast metabolism. *Nat. Genet.* **37**, 77–83.
- Shannon, P., *et al.* (2003). Cytoscape: A software environment for integrated models of biomolecular interaction networks. *Genome Res.* **13**, 2498–2504.
- Sheff, M. A., and Thorn, K. S. (2004). Optimized cassettes for fluorescent protein tagging in *Saccharomyces cerevisiae*. *Yeast* **21**, 661–670.
- Sopko, R., *et al.* (2006). Mapping pathways and phenotypes by systematic gene overexpression. *Mol. Cell* **21**, 319–330.

- Sopko, R., *et al.* (2007). Activation of the Cdc42p GTPase by cyclin-dependent protein kinases in budding yeast. *EMBO J.* **26**, 4487–4500.
- St Onge, R. P., *et al.* (2007). Systematic pathway analysis using high-resolution fitness profiling of combinatorial gene deletions. *Nat. Genet.* **39**, 199–206.
- Tanaka, M., *et al.* (2005). An unbiased cell morphology-based screen for new, biologically active small molecules. *PLoS Biol.* **3**, e128.
- Tong, A. H., *et al.* (2001). Systematic genetic analysis with ordered arrays of yeast deletion mutants. *Science* **294**, 2364–2368.
- Tong, A. H., *et al.* (2004). Global mapping of the yeast genetic interaction network. *Science* **303**, 808–813.
- Tong, A. H., and Boone, C. (2006). Synthetic genetic array analysis in *Saccharomyces cerevisiae*. *Methods Mol. Biol.* **313**, 171–192.
- Vizeacoumar, F. J., *et al.* (2009). A picture is worth a thousand words: Genomics to phenomics in the yeast *Saccharomyces cerevisiae*. *FEBS Lett.* **583**, 1656–1661.
- Vizeacoumar, F., *et al.* (2010). Integrating high-throughput genetic interaction mapping and high-content screening to explore yeast spindle morphogenesis. *J. Cell Biol.* **188**, 69–81.
- Waddington, C. H. (1957). *The Strategy of the Gene*. Allen and Unwin, London.
- White, S. A., and Allshire, R. C. (2008). RNAi-mediated chromatin silencing in fission yeast. *Curr. Top. Microbiol. Immunol.* **320**, 157–183.
- Winzeler, E. A., *et al.* (1999). Functional characterization of the *S. cerevisiae* genome by gene deletion and parallel analysis. *Science* **285**, 901–906.
- Wood, V., *et al.* (2002). The genome sequence of *Schizosaccharomyces pombe*. *Nature* **415**, 871–880.
- Ye, P., *et al.* (2005). Gene function prediction from congruent synthetic lethal interactions in yeast. *Mol. Syst. Biol.* **1**, 2005.0026.
- Zhu, H., *et al.* (2001). Global analysis of protein activities using proteome chips. *Science* **293**, 2101–2105.